J Mater Sci (2011) 46:1789–1795
DOI 10.1007/s10853-010-5002-6

Microstructure and mechanical properties of V–Ti–N microalloyed steel used for fracture splitting connecting rod

Xianzhong Zhang · Qizhou Cai · Guifeng Zhou · Qingfeng Chen · Yuzhang Xiong

Received: 29 May 2010 / Accepted: 11 October 2010 / Published online: 26 October 2010

Abstract A new kind of V–Ti–N high strength microalloyed medium carbon steel has been developed, which is used for fracture splitting connecting rod. In this article, the characteristics of this carbon steel and its production process were studied. The microstructure, precipitated phases and their effects on mechanical properties were investigated by optical microscope, SEM, and TEM. The results showed that the steel was constituted of ferrite and pearlite. By reducing the finish rolling temperature and accelerating the cooling rate after rolling, microstructure with fine grain ferrite and narrow lamellar space pearlite could be obtained in V–Ti–N microalloyed medium carbon, and a large number of precipitated phases distributed over ferrite. These led the tensile strength to be more than 1000 MPa, yield strength (YS) more than 750 MPa. The impact fractograph showed typically brittle fracture characteristic.

Introduction

The development of fracture splitting technology used for automobile engine connecting rod has been one of the significant advances in the 1990s [1–3]. Compared with the traditional method, it is beneficial to shortening the working procedures, minimize the processing equipments, and reduce the cost for producing connecting rod. The technology has first been applied extensively in Europe and North America, and some microalloyed carbon steels such as SPLITASCO70 and SPLITASCO50 (France), S53CVFS and S50CVS1 (Japan) and C70S6BY (Germany), etc., have been developed and used in the production of fracture splitting connecting rods [4]. However, they have not been widespread used because of low strength grades (SPLITASCO70, SPLITASCO50, S53CVFS, S50CVS1) or poor machinability (C70S6BY). In general, the microalloyed carbon steel used for automobile engine fracture splitting connecting rod requires high strength both in tension and compression, low distortion on fracture splitting, appropriate brittleness, and high sulfur for improved machinability. The desire strength can be obtained by changing the chemical composition, deformation temperature, and cooling rate during production [5, 6]. Decreasing the deformation temperature leads to the refinement of the prior austenite grains, which refines the final microstructure [7, 8]. The cooling rate after finish rolling also has effect on the microstructure and formation of precipitated phase of microalloyed steels [9]. On accelerated cooling the decrease of austenite to ferrite transformation temperature encourages ferrite nucleation at the austenite grain boundaries and in the grain interior. The enhanced nucleation rate restricts grain growth due to impingement of inter and intragranular ferrite leading to ferrite grain refinement [10–12]. At the same time, a higher cooling rate after finish rolling leads to a great deal of fine precipitations and effect the final microstructure and mechanical properties of microalloyed steels [13].

Addition of vanadium, titanium, and nitrogen to medium carbon steels increases strength levels through refining grain size and precipitation strengthening. In a given conditions, in V–Ti–N microalloyed medium carbon steels, the carbonitrides such as VC, V(C, N), TiN, and Ti(C, N) can

X. Zhang (✉) · Q. Cai
State Key Laboratory of Material Processing and Die and Mould Technology, Huazhong University of Science and Technology, Wuhan 430074, China
e-mail: zhangxianzh@hotmail.com

X. Zhang · G. Zhou · Q. Chen · Y. Xiong
Research and Development Center Wuhan Steel and Iron (Group) Co, Wuhan 430081, China

precipitate during hot deformation process. In general, the composition and stability of carbonitride depend on alloy composition of steel and hot deformation processing parameters [14–16]. Till now, more studies have previously been devoted to flat products produced from V, Nb, Ti–N microalloyed steels on strip and plate mills [17]. Different approaches have been used successfully for flat rolled products through controlling the microalloying elements contents of V, Nb, Ti, N and TMCP (Thermo-mechanical Control Process), which is used in low carbon microalloyed steel (≤0.20% C). The long products of microalloyed medium carbon steels have received limited attention in the literature, especially the effect on microstructure and properties of rolling processes.

The objective of this study is to study the effects of different rolling processes in V–Ti–N microalloyed medium carbon steel on microstructure and mechanical properties, including the fracture splitting properties through impact test.

Experimental procedure

The chemical composition of V–Ti–N microalloyed medium carbon steels used in this research is shown in Table 1. The steel was molten in 70 tons consteel electric arc furnace, refined in 70 tons ladle furnace, and continuously casted to 200 × 200 × 9000 mm billets. The billets were reheated in the regenerative furnace, and then rolled to rods with the diameter of 55 mm through controlled-rolling and accelerated cooling. Two kinds of processes were used in hot-rolling as shown in Table 2.

Specimens for metallographic examination were cut from the hot-rolled bars in the transverse direction. They were mechanically ground, polished, and etched in 4% nital for microstructure observation under an optical microscope. Microstructure was studied using OLYMPUS PME3-323UN optical microscope, and the volume fracture of ferrite was calculated using a systematic point count method by Leica image analysis instrument. Grain size of ferrite was estimated in terms of mean intercept length L_α determined using the following expression:

$$L_\alpha = (V_\alpha \times L)/N_\alpha \quad (1)$$

where V_α is the volume fracture of ferrite, N_α is the number of ferrite grains intercepted by the test lines, and L is the line length of the test lines.

Table 1 Chemical composition of V–Ti–N microalloyed steel (wt%)

C	Si	Mn	P	S	Cr	V	Ti	N
0.36	0.66	1.00	0.010	0.045	0.27	0.26	0.013	0.0110

Table 2 Hot-rolling processes

Process	Reheating temp/°C	Entry temp of finish rolling/°C	Finish temp/°C	Cooling rate/°C/s
1	1200	980	950	1.5
2	1200	980	930	15

The microstructure and lamellar spacing of pearlite were examined with Quanta 400 SEM. The samples were ground, polished, and etched in 4% nital. Each sample involved measurements of at least average five pearlite colonies fields of view and not less than 10 lamella of pearlite. The mean true spacing was measured and statistic calculated using a kind of measure software by Quanta 400 SEM. Carbon extraction replicas for transmission electron microscopy were prepared as following: polishing using diamond paste of 2 μm, etching in 3% nital solution (containing 3 vol% HNO_3), carbon deposition, and ungluing in 10% nital solution (containing 10 vol% HNO_3). A JEM-2100 FXII type TEM was employed to investigate the precipitation phases, morphologies, and energy dispersive spectrum.

Tensile samples with diameter Φ10 mm were cut from the hot-rolled bars. The sample axis was perpendicular to the rolling direction. Tensile test was carried out on a Instron test machine at a cross head speed of 1 mm/min. Charpy impact samples of 10 × 10 × 55 mm dimensions with 3 mm V-notch were cut from the hot-rolled bars. The impact test was conducted with a JB-30B Charpy impact testing machine at 20 °C. The impact fractograph was examined by SEM (Quanta 400, FEI).

Results and discussion

Microstructure

The microstructure of V–Ti–N microalloyed medium carbon steel under as-received condition was shown in Fig. 1. The microstructure of specimen fabricated by Process 1 and Process 2 constituted of ferrite and pearlite. However, the high volume fraction of pearlite and finer grain size could be obtained in Process 2. Furthermore, a thin continuous network proeutectoid ferrite on the boundary of prior austenite grains was observed in specimen prepared by Process 2. In the SEM photos shown in Fig. 1b and d, the lamellar spacing of pearlite in Process 2 was narrower than that in Process 1, and there were many precipitates in ferrite matrix.

Table 3 showed the volume fraction of pearlite, mean linear intercept grain sizes of ferrite, and lamellar spacing of pearlite in the microalloyed steel under as-received

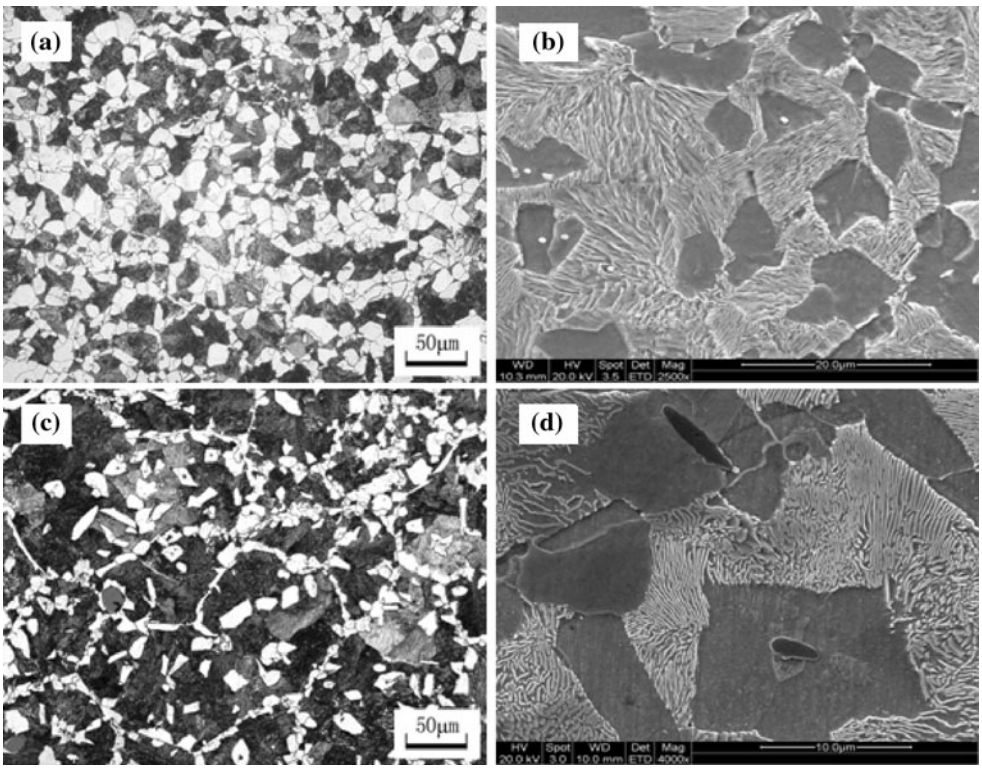

Fig. 1 Microstructure of V–Ti–N microalloyed medium carbon steel **a** Optical photo, Process 1; **b** SEM, Process 1;**c** Optical photo, Process 2; **d** SEM, Process 2

Table 3 Microstructure and grain dimension under the various rolling processes

Process	Microstructure	Percent of pearlite/%	lamellar spacing of pearlite/μm	Grain size of ferrite/ μm
1	Pearlite + ferrite	64	0.22	7.5
2	Pearlite + ferrite	74	0.19	6.0

condition. It was obvious that the volume fraction of pearlite increased approximately 15% and the mean linear intercept grain sizes of ferrite reduced approximately 20% by reducing the finishing rolled temperature and accelerating the cooling rate (Process 2). Furthermore, lamellar spacing of pearlite reduced 14% in Process 2.

The main difference between the Process 1 and Process 2 was deformation temperature during finish rolling and cooling rate after finish rolling. Decrease in the deformation temperature leads to a decrease of the austenite grain size and an increase of the degree of pancaking before transformation to ferrite. At these conditions, the transformation from austenite to ferrite or to pearlite is promoted due to the increase in nucleation sites at grain boundaries. Therefore, the finer ferrite grain sizes and shorter lamellar spacing of pearlite are obtained as is shown in Fig. 1.

The SEM observations showed that fine particles were precipitated in the ferrite (Fig. 1b and d), later identified as V(C, N) or (V, Ti) (C, N). After calculating with the IDS-model by Miettinen [18], the solution temperature of V(C, N) or (V, Ti) (C, N) is about 1260 °C, which is above the temperature of proeutectoid ferrite formation (Ar_3: 710 °C) and pearlite formation (Ar_1: 650 °C). In addition, the temperature of finish rolling (between 930 and 980 °C) is above Ar_3, so V(C, N) or (V, Ti) (C, N) precipitate before proeutectiod ferrite. However, it is well known that the solution ability of V(C, N) or (V, Ti) (C, N) in austenite is very large [19]. Only a few of volume fraction of V(C, N) or (V, Ti) (C, N) precipitates in austenite. The V(C, N) or (V, Ti) (C, N) particles restrict the prior austenite grain size and decrease the proeutectoid ferrite grain size because an increase in amount of grain boundaries improves proeutectoid ferrite nucleation.

Mechanical properties

The mechanical properties of V–Ti–N microalloyed medium carbon steel under various rolling processes were given in Table 4. As listed in Table 4, the bars with diameter of 35 mm by Process 2 showed higher YS, ultimate tensile strength (UTS), and yield ratio (YS to tensile strength) than that in Process 1. However, there were some decreases in elongation contraction of area and impact toughness.

Table 4 Mechanical properties under various rolling processes

Process	YS/MPa	UTS/MPa	Yield ratio/%	Contraction of area/%	Elongation/%	Room temperature impact energy/J
1	700	930	75.3	19.0	41.5	42
2	770	1010	76.3	18.0	36.0	37

In order to investigate the effects on the precipitate morphology, type, and size, a study was carried out, using TEM, with the investigated steels by different cooling processes after finish rolling. A lot of nitrides or carbonitrides scatter over ferrite matrix as shown in Fig. 2. They are small particles with size of less than 100 nm. EDS analysis indicates that the particles of less than 30 nm in diameter mainly are V(C, N) precipitations, and the particles of 30–100 nm in diameter are (V, Ti) (C, N) precipitations(Fig. 2). Furthermore, the volume fraction of precipitate particles of steel in Process 2 was more than that in Process 1. The grain sizes were also finer. Because as the cooling rate decreased, particle coarsening and growth occurred, causing a reduction in the number of particles/unit area [20].

For medium carbon microalloyed steel, the higher strength is attributed to: (1) solid solution strengthening, (2) remarkable grain refinement in the ferrite, (3) narrower lamellar spacing of pearlite, (4) more effective precipitation hardening, and (5) higher dislocation densities in the ferrite. Its strength depends on the chemical composition, deformation temperature during rolling and cooling rate after finish rolling.

Because certain amount of V(C, N) or (V, Ti) (C, N) still dissolved in the austenite during finish rolling (The temperature of finish rolling is between 930 and 980 °C, as shown in Table 2.), the cooling rate after finish rolling has great effect on precipitation of V(C, N) or (V, Ti) (C, N) from austenite, proeutectoid ferrite, or pearlite. Usually, precipitation of the V(C, N) or (V, Ti) (C, N) takes place in two different ways. One is the so called inter-phase precipitation where nucleation occurs on the austenite–ferrite phase boundary, producing a particle-rich sheet at the location where the boundary is temporarily halted. The carbonitride particles continue to grow until another ferrite ledge passes over them, and the process is repeated [21]. This precipitation mode which appears as rows of particles in TEM is only possible at relatively high transformation temperatures. A typical feature is also that the rows of particles are formed in the same region and the same orientation, a unique variant of the Baker–Nutting (B–N) orientation relationship with the ferrite matrix [22]. The other is homogeneous nucleation and growth of the carbonitrides. It may occur in the newly formed ferrite, notably at lower transformation temperatures. In this case, the particles are not aligned in rows but randomly distributed. They are also characterized by the occurrence of different variants of the B–N orientation relationship [23]. Figure 2 indicates that there is no tendency for precipitate row formation. For the two processes, which are showed in Table 2 relevant to the present discussion, the precipitates are randomly distribution, either nucleated homogeneously in the matrix or on dislocations in the ferrite structures. However, the Process 2 results in more volume fraction and finer V(C, N) or (V, Ti) (C, N) than Process 1. This results in precipitation strengthening.

The ferrite grain size, lamellar spacing of pearlite, and precipitations have effected on impact toughness. As shown in Table 4, there is a decrease of impact toughness in Process 2 than Process 1. These may relate to the thin continuous network proeutectoid ferrite (Fig. 1) and more volume fraction of precipitations in Process 2.

Impact fracture surface analyzing

The impact fracture surfaces of V–Ti–N medium carbon microalloyed steel were studied using SEM. The results were shown in Fig. 3. The impact fracture surface is even without dimple and necking in the core, which shows distinct brittle fracture character (Fig. 3a and b). Cleavage region has also seen a number of particles and strip MnS inclusions, whose morphologies and energy spectra are shown in Fig. 3c, the other can be seen mixed with a small amount of carbonitride particles and some with oxide particles, shown in Fig. 3d and e.

One of the properties require for the fracture splitting connecting rods is that shape and dimension of the connecting rod after assembly do not change during processing. Moreover, it is required to have a precise positioning within microns by facing the fracture surface to assemble the cap and the rod. Therefore, the fracture surface is required to undergo brittle fracture. According to the impact fracture surface of the developed V–Ti–N medium carbon microalloyed steel, it is easy to obtain a brittle fracture due to the high strength and certain amount of MnS, a small amount of carbonitride particles and some with oxide particles, which can become the cleavage initiation.

Conclusions

(1) For V–Ti–N microalloyed medium carbon steel, grain size of ferrite, pearlite group, and lamellar spacing of

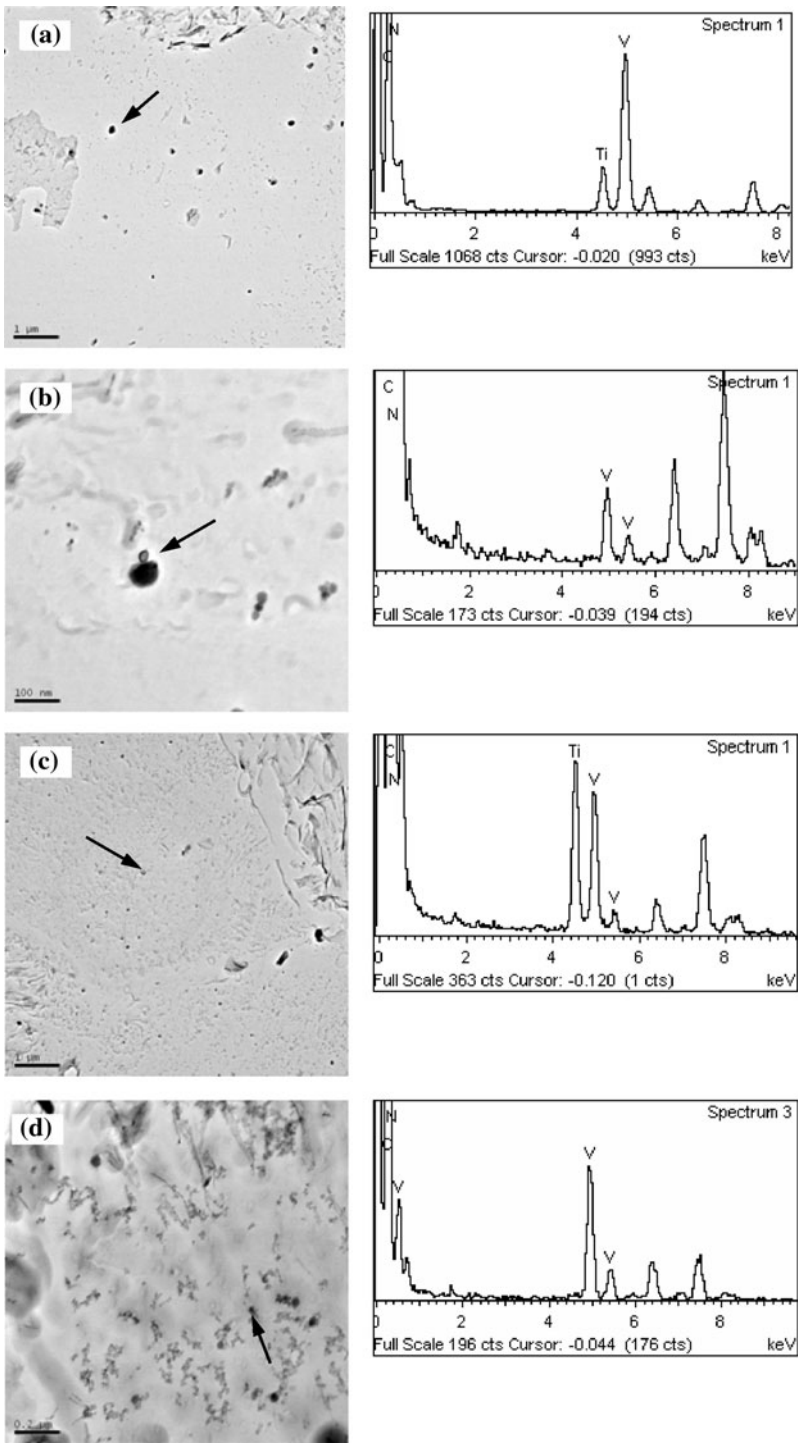

Fig. 2 TEM and EDS of the precipitation phases in case of different rolling process, **a** (V, Ti) (C, N) precipitations, Process 1; **b** V(C, N) precipitations, Process 1; **c** (V, Ti) (C, N) precipitations, Process 2; **d** V(C, N) precipitations, Process 2

pearlite could be fined by reducing the finish rolling temperature and accelerating cooling rate. More volume fraction of pearlite could be obtained as well. At the cooling rate of 15 °C/s, the grain size of ferrite was 6.0 μm, the volume fraction of pearlite was 74%, and lamellar spacing of pearlite was 0.190 μm.

(2) More volume fraction and finer grain sizes of nitrides or carbonitrides could be obtained at high cooling rate of 15 °C/s. This resulted that the tensile strength could be more than 1000 MPa and YS could be more than 750 MPa, which were both beneficial to the need of connecting rod materials.

(3) The impact fracture surfaces showed a characteristic of typically brittle fracture. Sulfides, carbonitrides, and oxide particles could become the cleavage initiation.

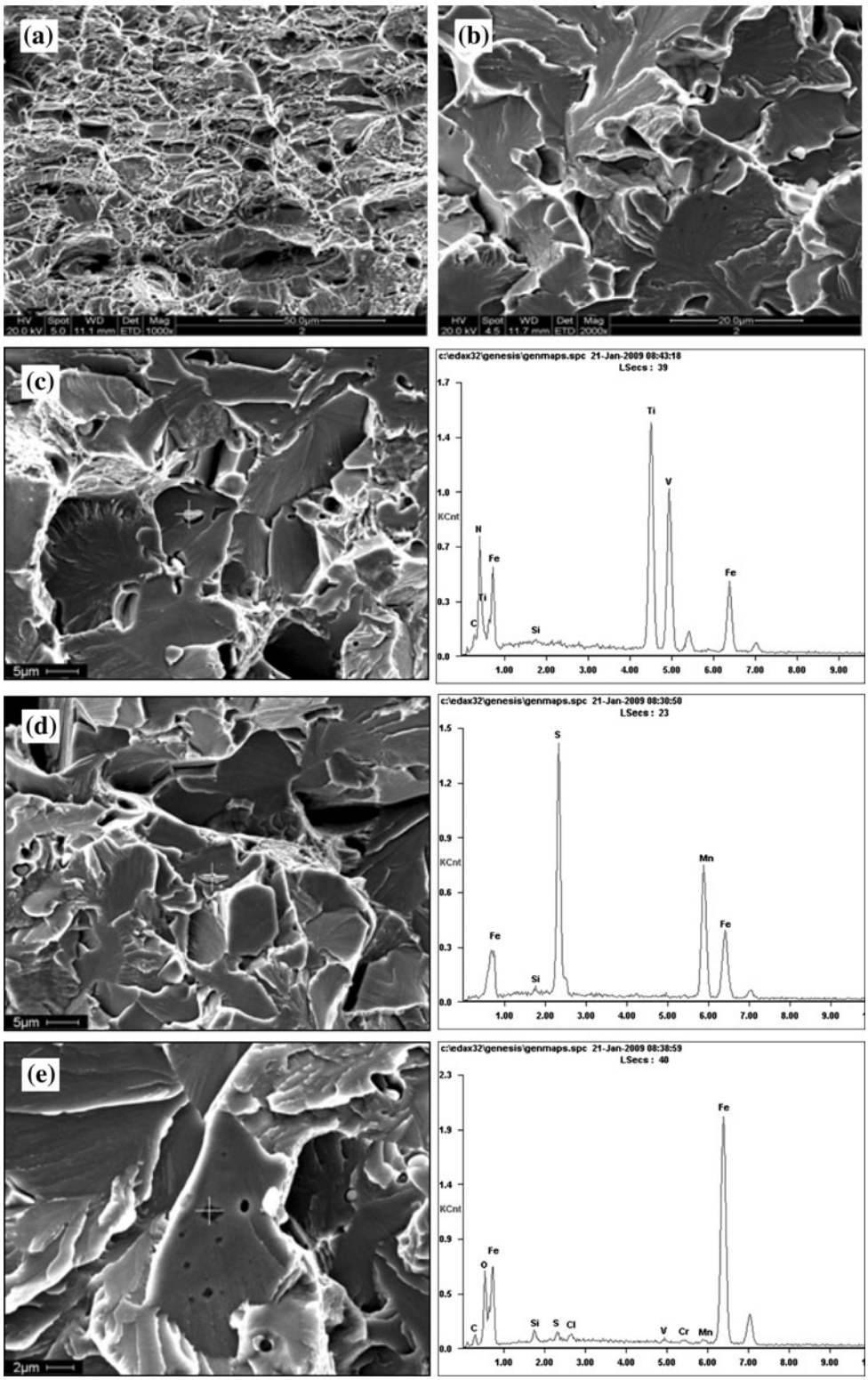

Fig. 3 SEM of Charpy fracture surface

References

1. Gu Z, Yang S, Ku S, Zhao Y, Dai X et al (2005) Int J Adv Manuf Technol 25:883
2. Yu R (1998) Process Mater Automob 9:9
3. Kou S, Yang S, Deng C et al (2001) Chin Mech Eng 12(7):83
4. Cristinacce M, Reynolds PE, Milbourn DJ et al (1996) The second international symposium on microalloyed bar and forging steel. Colorado School of Mines, Colorado, p 1
5. Naylor DJ (1998) Mater Sci Forum 284-286:83
6. Matlock DK, Krauss G, Speer JG (2001) J Mater Process Technol 117:324
7. Gonzalez-Baquet I, Kaspar R, Richter J (1997) Steel Res 68(2):61
8. Jahazi M, Eghbali B (2001) J Mater Process Technol 113:594
9. Shanmugam S, Ramisetti NK, Misra RDK et al (2007) Mater Sci Eng A 460–461:335
10. Li Z, Wu D, Lv H-S, Fang S-R (2007) J Iron Steel Res 14(5):277
11. Ai JH, Zhao TC, Gao HJ et al (2005) J Mater Process Technol 160(3):390
12. Cota AB, Barbosa R, Santos DB (2000) J Mater Process Technol 100(1–3):156
13. Liu S-X, Chen Y, Liu G-Q et al (2008) Mater Sci Eng A 485:492
14. Loberg B, Nordgren A, Strid J, Easterling KE (1984) Metall Mater Trans A 15(1):33
15. Strid J, Easterling KE (1985) Acta Metall 33(2):2057
16. Suzuki S, Weatherly GC, Houghton DC (1987) Acta Metall 35(2):341
17. Williams JG, Killmore CR, Barbaro FJ, Meta A, Fletcher L (1995) In: Korchynsky M (ed) Proceedings of international conference on microalloying 95. ISS, Pittsburgh, p 117
18. Miettinen J (1996) Ironmak Steelmak A 23(4):346
19. Lagneborg R, Siwecki T, Zajac S, Hutchinson B et al (1999) Scand J Metall 28:186
20. Bepari MA (1990) Mater Sci Technol 6:338
21. Strid J, Easterling KE (1985) Acta Metall 33:2057
22. Satoshi K, Ryuji O (2006) Jpn Automob Manuf Assoc 20:7
23. Shanmugam S, Tanniru M, Misra RDK, Panda D, Jansto S et al (2005) Mater Sci Technol 21(2):165